

Provided for non-commercial research and education use.
Not for reproduction, distribution or commercial use.



This article appeared in a journal published by Elsevier. The attached copy is furnished to the author for internal non-commercial research and education use, including for instruction at the authors institution and sharing with colleagues.

Other uses, including reproduction and distribution, or selling or licensing copies, or posting to personal, institutional or third party websites are prohibited.

In most cases authors are permitted to post their version of the article (e.g. in Word or Tex form) to their personal website or institutional repository. Authors requiring further information regarding Elsevier's archiving and manuscript policies are encouraged to visit:

<http://www.elsevier.com/authorsrights>



Contents lists available at SciVerse ScienceDirect

Computational Materials Science

journal homepage: www.elsevier.com/locate/commatsci

Surface and interface controlled yielding and plasticity in fivefold twinned Ag nanowires

Mingfei Sun^a, Ronggen Cao^a, Fei Xiao^a, Chuang Deng^{b,*}^a Department of Materials Science, Fudan University, 220 Handan Road, Shanghai 200433, China^b Department of Mechanical and Manufacturing Engineering, The University of Manitoba, 15 Gillson Street, Winnipeg, MB R3T 5V6, Canada

ARTICLE INFO

Article history:

Received 25 March 2013

Received in revised form 31 May 2013

Accepted 10 June 2013

ABSTRACT

Molecular dynamics simulations are used to investigate the influences of pre-existing microstructural defects on the strength and deformation mechanisms in Ag nanowires under both uniaxial deformation and nanoindentation. In particular, the synergistic effects from both internal and external structural defects, including twin boundaries, surface facets, and a special surface groove, are studied. It is found that the yielding modes vary among Ag nanowires when different microstructures are present. Furthermore, while fivefold twin boundaries are found to cause significant strain hardening under nanoindentation, they can either decrease or increase the initial yield stress of Ag nanowires under uniaxial deformation. The surface groove, in addition, will result in damping behavior of the Ag nanowire that leads to peculiar oscillating load–displacement responses under nanoindentation.

© 2013 Elsevier B.V. All rights reserved.

1. Introduction

Metal nanowires (NWs) have been extensively studied in recent years because of their potential applications as building blocks in micro-electro-mechanical systems [1,2] and optoelectronics [3,4]. Due to their limited size and high surface-to-volume ratio, it has been widely observed from both *in situ* nanomechanical tests [5,6] and atomistic simulations [7–10] that the yielding and plasticity in metal NWs were dominated by free surfaces and possible internal structural defects, e.g., grain boundaries. This is in sharp contrast to conventional bulk materials in which the mechanical deformation is mainly controlled by dislocation activities within individual grains. Therefore, it is important to obtain a deep understanding of the influences of both internal and external microstructural defects on the mechanical properties of metal NWs under various loading environments so that their reliability can be assessed.

Various surface features and internal microstructures can form during the synthesis of metal NWs. For instance, Ag NWs could be either cylindrical [11] or pentagonal with flat surface facets [5,12] depending on the synthesis conditions. In addition, internal structural defects such as coherent twin boundaries (CTBs) with fivefold symmetry (known as fivefold twinning) were frequently observed in both cylindrical [11] and pentagonal [12,13] Ag NWs. Fivefold twinned (FT) crystal structures are common defects found in

face-centered cubic (FCC) metals [12–15]. However, it is known that the five subunits of theoretical angle in FT structure cannot form a closed space-filling wire, resulting in substantial internal strain [12–14]. Based on lattice crystallography, the theoretical angle between adjacent {1 1 1} twin boundaries in FT NWs is 70.53°, which generates a 7.53° angular deficiency [12,13]. While such angular deficiency suggests that most FT NWs synthesized from experiments were inherently strained, it also implies that a surface groove may form in FT NWs in order to reconcile the strain. This speculation was recently confirmed in experiments by Zhang et al. [13], who successfully synthesized pentagonal FT Ag NWs with re-entrant grooves on the surface. They found that the grooves were closely related to the relaxation of the inherent strain, which was believed to be the restriction of the lateral growth in these NWs [13]. Similar surface groove was also observed in FT boron carbide NWs [16]. Since the mechanical properties of metallic NWs largely depend on the free surfaces, strain relaxation caused by the formation of a surface groove in FT Ag NWs may significantly impact their mechanical properties.

Furthermore, CTBs are special interfaces of low energy that can serve as strong barriers to defects which have been confirmed by both experiments [17,18] and atomistic simulations [7,8,19]. For example, Au NW with a high density of parallel nanoscale CTBs has been found from molecular dynamics (MD) [7,8] to exhibit higher tensile strength than single crystalline Au NWs of similar sizes. What is more, twinned Au NWs with special zigzag surface facets have been predicted by MD to approach the ideal strength in Au [8]. Nevertheless, only limited experimental studies and atomistic simulations have been performed in the past regarding

* Corresponding author. Tel.: +1 204 272 1662.

E-mail address: dengc@ad.umanitoba.ca (C. Deng).

fivefold CTBs in metal NWs. Wu et al. [11] have found from bending experiments that FT Ag NWs were stronger but more brittle than twin-free Ag NWs. Similar results have been obtained from MD by studying the tensile [20–23] and torsional [21] deformations of FT Ag NWs. However, the synergy between surface features and internal CTBs on the yielding of FT Ag NWs has not been fully explored. In particular, the mechanical properties of metal NWs with the recently observed surface groove [13] have not been investigated from either experiments or atomistic simulations. In addition, the deformation of FT Ag NWs under other loading conditions, e.g., uniaxial compression and nanoindentation [24,25], which is a direct mechanical characterization of the FT NW surface, needs to be studied so that the fundamental mechanisms of deformation and plasticity in FT NWs can be justified.

The aim of this work is to elucidate the deformation process of FT Ag NWs with re-entrant surface groove subjected to uniaxial deformation and nanoindentation by MD simulations. A comparative study of the atomistic insight into the plasticity of twin-free single-crystalline (SC) Ag NW, FT Ag NW and FT Ag NW with surface groove is presented. The role of surfaces facets, fivefold twin boundaries, and surface groove on the yielding and plasticity of Ag NWs is discussed respectively.

2. Simulation methodology

The simulations were performed using LAMMPS [26] with a time step of 5 fs. The interatomic interactions were characterized by an embedded atom method potential developed for Ag [27]. The axis of all Ag NWs was oriented along $\langle 110 \rangle$ direction (Fig. 1). Periodic boundary conditions were applied along the NW axis while other directions were kept free. According to Zhang et al. [13], a gap (surface groove formed during crystal growth) was constructed with the two wedge surfaces parallel to the twin boundaries. The groove size G was defined as in Fig. 1b and Ag NWs with two different groove sizes, $G = 5$ nm and $G = 7.5$ nm, were investigated. The diameter was 20 nm and the length was 50 nm for all Ag NWs. Pentagonal FT Ag NW with or without surface groove was constructed by cutting the respective cylindrical NW with flat facets (Fig. 1b). The NW visualization was done by AtomEye [28]. The system temperature was kept at 10 K during all simulations by using NVT (constant temperature, constant volume) integration scheme with Nose–Hoover thermostat. All NWs were relaxed at 10 K for 500 ps before indentation or uniaxial deformation was performed. After relaxation, uniaxial tension or compression was performed by uniformly deforming the NWs at a constant strain rate of 10^8 s^{-1} under NVT.

Nanoindentation was simulated by moving a spherical virtual indenter at a constant velocity of 1 m/s towards the sample surface (Fig. 1a). In SC Ag NW, the indentation was performed along the $\langle 001 \rangle$ crystallographic direction (Fig. 1b). In FT Ag NWs, two indentation directions were used: one was towards the free surface along the $\langle 001 \rangle$ direction as similar to that in SC Ag NW, and the other was towards the twin boundary. The indentation directions were indicated by black arrows in Fig. 1b.

A repulsive force $f(r)$ was exerted by the indenter according to the following equation:

$$f(r) = K(r - R)^2, \quad (1)$$

where $f(r)$ is the repulsive force, R is the radius of the indenter ($R = 10$ nm), r is the distance from the atom to the center axis of the indenter, and K is the specified force constant ($K = 100 \text{ eV nm}^{-1}$). Several atomic layers of each NW were fixed on the surface opposite to the indentation direction. For each Ag NW, the indentation stopped when the depth (h) reached 4.5 nm.

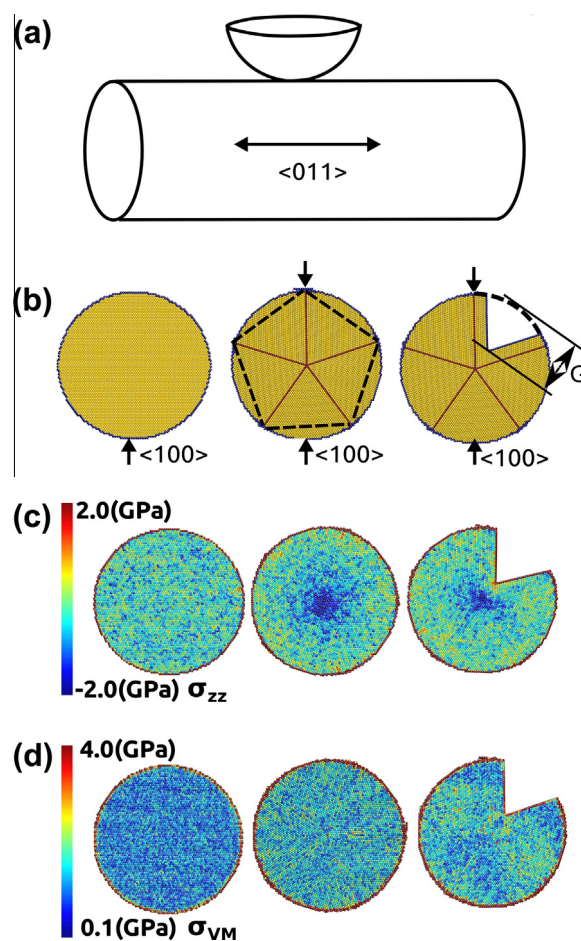


Fig. 1. (a) Schematic model of uniaxial deformation and spherical nanoindentation of Ag NWs. (b) Atomistic configuration of the cross-section of SC Ag NW, FT Ag NW, and FT Ag NW with surface groove of size G . The arrows indicate the contact position and indentation direction of each Ag NW. Initial distribution of (c) axial stress (σ_{zz}) and (d) von Mises stress (σ_{VM}) of relaxed Ag NWs prior to indentation. In (b), the atom colors correspond to local lattice structure. In (c), the atom colors correspond to atomic stress along the axial direction. The axis of all NWs is oriented along $[110]$ direction. (For interpretation of the references to color in this figure legend, the reader is referred to the web version of this article.)

3. Results

3.1. Initial stress distribution

After the initial relaxation, the atomic level axial stress (σ_{zz}) and von Mises stress (σ_{VM}) in cylindrical Ag NWs prior to any deformation were analyzed and shown in Fig. 1c and d, respectively. For simplicity, the result for FT Ag NW of groove size $G = 5$ nm was not shown which was similar to that of groove size $G = 7.5$ nm. The analysis of axial stress (σ_{zz}) has been widely used in the past to investigate the yielding of metal NWs under uniaxial deformation and a strong correlation has been found between the initial distribution of axial stress σ_{zz} and the yielding behavior of metal NWs [9,29–31], e.g., the dislocation nucleation site [31] and the asymmetric yield strength in metal NWs under uniaxial tension and compression [29].

It was found from Fig. 1c that the distribution of axial stress σ_{zz} differed markedly among the three types of Ag NWs. While the interior of all NWs showed compressive stress (as indicated by blue atoms in Fig. 1c), the stress level was the highest in the groove-free FT Ag NW and the lowest in the SC Ag NW. These findings agreed well with Wu et al. [20] that fivefold CTBs can cause

excessive internal compressive stress in FCC Fe NWs. With the presence of a surface groove (Fig. 1c), it can be seen that the internal compressive stress was partially relaxed as compared to the groove-free FT Ag NW but remained higher than that in the SC Ag NW. On the other hand, as shown in Fig. 1d, the influences of a surface groove on the distribution of von Mises stress (σ_{VM}) in FT Ag NWs were subtle. It is also noted that the quincifoliate flower pattern along the fivefold CTBs that has been found by Wu et al. [20] can be barely seen in the FT Ag NWs in Fig. 1d, which might be due to the reasons that FCC Fe NWs at 0.01 K were studied by Wu et al. [20] and Ag NWs at 10 K were studied in this research.

3.2. Uniaxial deformation

The stress–strain response in each Ag NW under both uniaxial tension and compression was plotted in Fig. 2a and b, respectively. All curves showed a sharp yielding phenomenon; the stress dropped dramatically after a critical value was reached. The yield stress (σ_y) of each Ag NW which was defined as the maximum stress on the stress–strain curve was listed in Fig. 2.

It is shown from Fig. 2a and b that fivefold twinning led to distinct effects in Ag NWs under tension and compression. During uniaxial tension, the yielding in all FT Ag NWs occurred at relatively higher stresses but significantly earlier than that in SC Ag NW; e.g., the FT Ag NW yielded at the strain of ~ 0.12 and the stress of $\sigma_y = 3.65$ GPa while the SC Ag NW yielded at the strain of ~ 0.18 and the stress of $\sigma_y = 3.40$ GPa. All things considered, fivefold twinning resulted in an increased elastic modulus and decreased ductility in Ag NWs under uniaxial tension. These results were in line with past simulations [20,21]. The influence from surface groove, however, was somewhat moderate; only slight decrease of the yield stress was caused by the presence of a surface groove in FT Ag NWs regardless of the groove size.

In contrast, while the elastic modulus was more or less the same among all Ag NWs under uniaxial compression (Fig. 2b), the FT Ag NWs were significantly weaker than the SC Ag NW. In particular, the compressive yield stress in the FT Ag NW ($\sigma_y = 8.47$ –9.32 GPa) was more than 1 GPa lower than that in the SC Ag NW ($\sigma_y = 9.67$ GPa). It is also important to note that the surface grooves

caused slight increase in the compressive yield stress in FT Ag NWs, which is the opposite to tensile results.

The strengthening effects during tension and weakening effects during compression caused by fivefold CTBs in Ag NWs can be well explained by the initial stress distribution as found previously in Fig. 1c. Specifically, the high initial compressive stress prior to deformation in FT Ag NWs made it easier for them to yield under compression and more difficult to yield under tension than in SC Ag NWs. Furthermore, since the surface groove can partially relax the initial compressive stress in FT Ag NW (Fig. 1c), the yield stress in FT Ag NW with surface groove was found to be between that in SC Ag NW and perfect FT Ag NW under both tension and compression.

In order to understand how the yielding occurred, the atomistic configurations at the yield point of each Ag NW were shown in Fig. 2c and d for tensile and compressive deformations, respectively. In these figures, the atom colors correspond to local lattice structure and perfect FCC atoms have been removed for clarity. For simplicity, only the results for perfect FT Ag NW and FT Ag NW with surface groove size of $G = 7.5$ nm were shown. It was found that the groove size did not affect the yielding mechanisms.

The yielding of SC FCC NWs under both uniaxial tension and compression has been widely studied in the past [7,9,29]. In SC FCC NWs under uniaxial tension, the yielding was initiated by nucleation of a Shockley partial dislocation from the free surface [29]. On the other hand, the yielding was caused by consecutive nucleation of leading and trailing Shockley partial dislocations under uniaxial compression in SC FCC NWs [29]. In FT Ag NWs, although the yielding was also caused by nucleation of Shockley partial dislocations from the surface (as indicated by the dashed circles in both Fig. 2c and d), the locations of nucleation site were found to be closely related to the internal CTBs and surface groove. For instance, for FT Ag NWs under uniaxial tension (Fig. 2c), the dislocation nucleation was found to start specifically from the intersection between the CTB and free surface in spite of the presence of surface grooves. Under uniaxial compression (Fig. 2d), however, the dislocation nucleation in FT Ag NW was no longer from the CTB–surface interaction. Furthermore, when a surface groove was present, the dislocation was found to nucleate specifically from the groove tip at the yield point under compression.

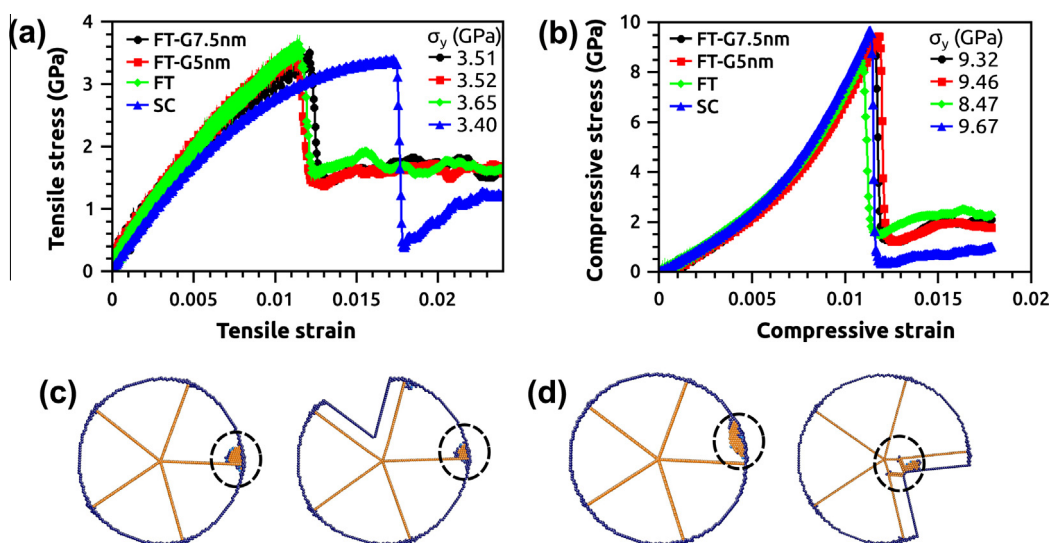


Fig. 2. (a) Tensile and (b) compressive stress–strain curves of various Ag NWs. Atomistic configurations of FT Ag NWs at the yield points under (c) tension and (d) compression. The yield stress (σ_y) is defined as the maximum stress from the stress–strain curves. The atom colors correspond to local lattice structure and perfect FCC atoms have been removed for clarity. The black dashed circles indicate the dislocation nucleation sites at the yield points. (For interpretation of the references to color in this figure legend, the reader is referred to the web version of this article.)

3.3. Nanoindentation

The indentation force (p) vs. indentation depth (h) for each Ag NW was plotted in Fig. 3. The indentation direction was indicated by the arrows in the inset of each figure, e.g., towards the free surface and twin boundary for Fig. 3a and b, respectively.

It is found from both Fig. 3a and b that during the early stage of the indentation, the indentation forces were more or less the same among all the Ag NWs regardless of the microstructures; the p – h curves were almost on top of each other before the indentation depth reached about $h \sim 1$ nm. As the indentation went on, the Ag NWs started to behave differently. For indentation towards the free surface when $h > 1$ nm, it is noted that the indentation forces in the SC Ag NW became significantly lower than the FT Ag NWs, which suggested strain hardening by CTBs in FT Ag NWs. Furthermore, it can be seen from both Fig. 3a and b that surface grooves can lower the indentation force in FT Ag NWs and the bigger the groove size, the lower the indentation force.

In order to demonstrate the strain hardening effects induced by fivefold CTBs, the representative atomistic configurations of Ag NWs at an indentation depth of $h \sim 1.7$ nm (as indicated by the vertical dashed lines) were presented in Fig. 3c and d, respectively; the indentation direction was indicated by black arrows in these figures. The perfect FCC atoms were removed for clarity. It is clearly shown from Fig. 3c and d that the plasticity was confined to local regimes outlined by CTBs in all FT Ag NWs. The dislocations were blocked by CTBs and could not move freely or transmit to neighboring subunits. This observation was consistent with past simulations that CTBs can serve as strong barriers to dislocation propagation in FCC metals and lead to strong strain hardening [19]. In contrast, the dislocations can easily escape from the free surface of SC Ag NWs (Fig. 3e) and cause significant softening.

Another interesting phenomenon noticed from Fig. 3 was the unusual oscillating behavior in the p – h curve of the FT Ag NWs with surface groove. For example, during the early stage of the indentation ($h < 1$ nm), clear spikes were observed on the p – h curves for FT Ag NW of groove size equal to 7.5 nm (FT-G7.5 nm, Fig. 3a and b). This is dramatically different from the smooth evolution p – h curves for Ag NWs without surface groove. Such

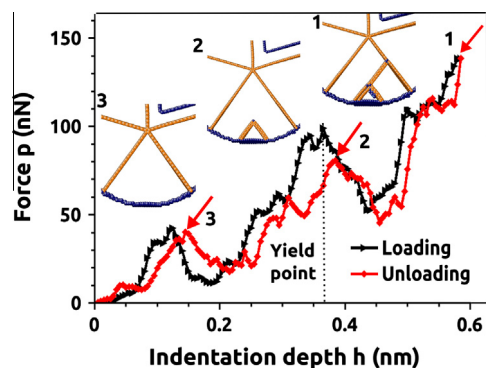


Fig. 4. Simulated loading–unloading curves of cylindrical FT Ag NW with surface groove under nanoindentation. The insets are atomistic configurations of the NW at different stages of unloading with atom colors corresponding to their local lattice structure. Perfect FCC atoms and part of the NW have been removed for clarity. The vertical dashed line indicates the initial yield point upon loading. (For interpretation of the references to color in this figure legend, the reader is referred to the web version of this article.)

behaviors were in-line with the observations that during the indentation, the surface groove can dissipate part of the applied energy through damping, or specifically, via the “opening-and-closing” of the surface groove. One movie showing the “opening-and-closing” behavior during the indentation of FT-G7.5 nm Ag NW has been included in Supplement materials.

While a sharp drop on the p – h curve during nanoindentation test normally indicates an event of yielding or dislocation emission in the tested material, the drop in p associated with the spikes in Fig. 3 was not necessarily an indication of such event in FT Ag NWs with surface groove. In order to clarify this point and demonstrate how fivefold CTBs can result in strain hardening, we presented in Fig. 4 a load–unload curve of FT-G7.5 nm Ag NW with indentation towards the free surface. Here the yielding was defined as the point at which the first dislocation was emitted. It is shown that the yielding occurred at the second spike ($h \sim 0.36$ nm, as marked by the vertical dashed line in Fig. 4) and no dislocation was nucleated

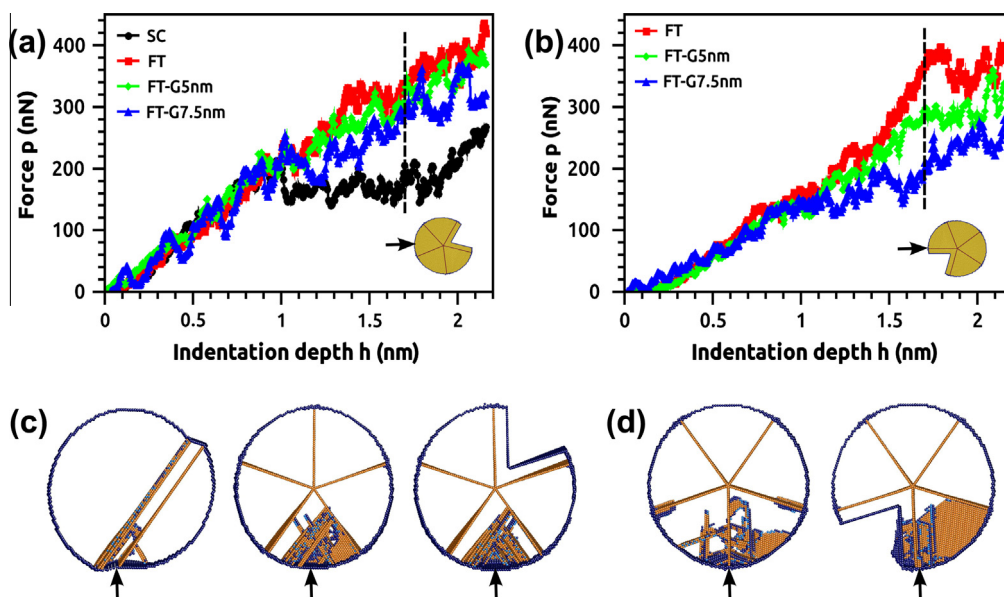


Fig. 3. (a) Force–displacement (p – h) responses with indentation towards the free surface of Ag NWs. (b) Force–displacement (p – h) responses with indentation towards the CTBs of Ag NWs. Atomistic configurations of Ag NWs at the indentation depth as marked by the vertical dashed lines in (a) and (b) for indentation towards (c) free surface and (d) twin boundaries, respectively. Atoms are colored according to their local lattice structure and perfect FCC atoms have been removed for clarity. The indentation direction is indicated by the black arrow in each figure. (For interpretation of the references to color in this figure legend, the reader is referred to the web version of this article.)

at the first spike ($h \sim 0.12$ nm). What is more, a complete plastic recovery during the unloading was observed; the loading and unloading curves almost overlapped each other. The atomistic configurations at different stages during the unloading (insets of Fig. 4) also confirmed that partial dislocations that were nucleated after the yield point gradually disappeared upon the unloading. The complete plastic recovery is in good agreement with past studies [7] on twinned Au NW under tensile deformation with subsequent unloading; it was found that the motion of leading partial dislocations would be hindered by CTBs and cause significant strain hardening until the trailing dislocations catch up and form full dislocations [7].

3.4. Influences of surface facets

Experimentally synthesized FT Ag NWs have been found to exist in both cylindrical [11] and pentagonal [13] forms. Therefore it is important to assess the effects of surface facets on the mechanical properties of FT Ag NWs. As similar to that for cylindrical FT Ag NWs, both uniaxial deformation and nanoindentation were simulated in pentagonal FT Ag NWs. As shown in Fig. 5, pentagonal FT Ag NWs with a surface groove (groove size $G = 7.5$ nm as defined in Fig. 1b) was also constructed and tested.

The distribution of initial axial stress (σ_{zz}) in both types of pentagonal FT Ag NW prior to any deformation was presented in Fig. 5a. As similar to the cylindrical FT Ag NW, the interior of perfect pentagonal FT Ag NW was also shown to be highly compressive, which can be partially relaxed by the presence of a surface groove. Furthermore, qualitative estimation based on comparison between Figs. 1c and 5a implies that the surface facets can cause additional compressive stress to the interior of the pentagonal FT Ag NWs.

Under uniaxial deformation, both types of pentagonal FT Ag NWs showed sharp yielding phenomenon as similar to that in cylindrical FT Ag NWs. The atomistic configurations at the yield point of each NW along with the yield stress (σ_y) were presented in Fig. 5b and c for uniaxial tension and compression, respectively. It is found that the yielding in all pentagonal FT Ag NWs was caused by the nucleation of Shockley partial dislocation from the intersection between CTB and the free surface regardless of the loading mode and surface feature. However, it needs to be

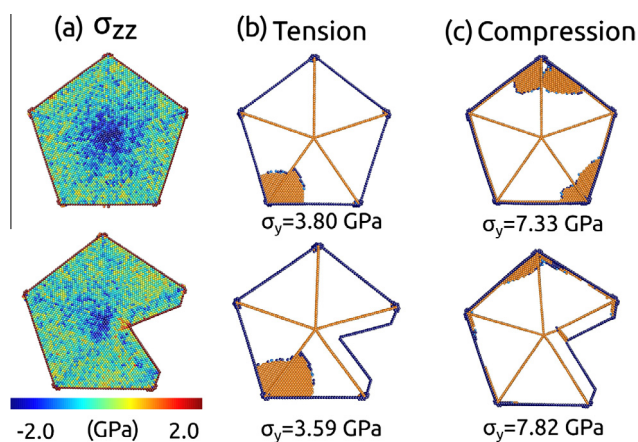


Fig. 5. (a) Initial stress distribution (σ_{zz}) of relaxed pentagonal FT Ag NWs prior to deformation. Atoms are colored according to atomistic stresses along the axial direction. Atomistic configurations of pentagonal FT Ag NWs at the yield points under uniaxial (b) tension and (c) compression. Atom colors correspond to local lattice crystal structure and perfect FCC atoms have been removed for clarity. The yield stress (σ_y) is defined as the maximum stress during the uniaxial deformation in each FT Ag NW. (For interpretation of the references to color in this figure legend, the reader is referred to the web version of this article.)

mentioned that in pentagonal FT Ag NW with surface groove, a Shockley partial dislocation was emitted at the groove tip (Fig. 5c) without causing significant drop of the stress well before the yield point was reached under compression. Such yielding mechanism differs from that observed in cylindrical FT Ag NW with surface groove, in which the yielding was caused by nucleation of Shockley partial dislocation from the tip of the surface groove.

Besides, by comparing the yield stresses listed in Fig. 5b and c and those in Fig. 2a and b, it is found that the surface facets led to moderate strengthening under tensile deformation (e.g., $\sigma_y = 3.8$ GPa and $\sigma_y = 3.65$ GPa in pentagonal and cylindrical FT Ag NWs, respectively) but severe weakening under compressive deformation (e.g., $\sigma_y = 7.33$ GPa and $\sigma_y = 8.47$ GPa in pentagonal and cylindrical FT Ag NWs, respectively) in Ag NWs. This is consistent with the increased initial compressive stress induced by surface facets in pentagonal FT Ag NWs as shown in Fig. 5a. Due to the partial relaxation of initial compressive stress with the presence of a surface groove, the yield stresses were lower in tension but higher in compression as compared to closed pentagonal FT Ag NW. Such observations were similar to those in Fig. 2a and b regarding cylindrical FT Ag NWs.

The indentation results (p - h curves) in both types of pentagonal FT Ag NWs were presented in Fig. 6a and b for indentation towards the free surface and twin boundary, respectively; the indentation position was indicated by the black arrow in the insets. Overall the indentation results were similar to those observed in cylindrical FT Ag NWs. For example, strong strain hardening effects were observed in all pentagonal FT Ag NWs; representative atomistic configurations at $h = 1.7$ nm (marked by the vertical dashed lines) showing confined dislocation activities by CTBs were included (insets of Fig. 6). Furthermore, the p - h curves for pentagonal FT Ag NW with surface groove showed a similar oscillating behavior to that observed in cylindrical Ag NWs.

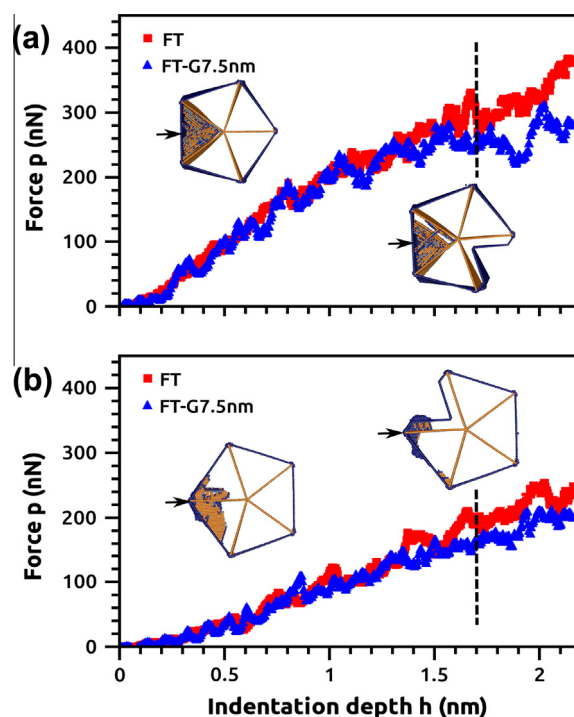


Fig. 6. Simulated force–displacement (p - h) curves in pentagonal FT Ag NWs with indentation towards (a) the free surface and (b) the twin boundaries. The inset shows the atomistic configuration of each Ag NW at the indentation depth marked by the vertical dashed line. The indentation position is indicated by the black arrow for each Ag NW.

4. Discussion

4.1. Yielding under uniaxial deformation vs. under nanoindentation

It is shown in Fig. 2 that Ag NWs regardless of the internal and external microstructures exhibited a sharp yielding phenomenon with no strain hardening under both uniaxial tension and compression. In contrast, strong strain hardening has been found in FT Ag NWs under nanoindentation, although the yielding in all types of NWs occurred via the same mechanism under both uniaxial deformation and nanoindentation, e.g., nucleation of Shockley partial dislocation from the NW surface.

It has been found from past MD simulations [19] that whether or not strain hardening can be caused in twinned FCC metal NWs under uniaxial deformation depends on two stresses: the stress required for dislocation nucleation (or, σ_y) and that for dislocation transmission across the CTBs (or, σ_T). If σ_y is greater than σ_T , the nucleated partial dislocation upon yielding would transmit directly across CTBs and result in sharp yielding (no strain hardening). On the other hand, if σ_y is lower than σ_T , the propagation of nucleated partial dislocations at the yield point will be blocked at CTBs, thus causing significant strain hardening. It was further confirmed that the relative magnitude of σ_y and σ_T depends on the loading rate, temperature, and the stacking fault energy of the metal NWs [19].

For FT Ag NWs shown in Fig. 2, the stress to nucleate Shockley partial dislocation from the intersection between CTB and free surface was so high that it exceeded the resistance of CTBs towards dislocation transmission. As a result, the partial dislocations nucleated at the yield point would instantly cross the CTBs which led to strain softening. In FT Ag NWs under nanoindentation, however, the yielding occurred at a relatively early stage as shown in Fig. 4 and the stress was not high enough to make the dislocations transmit the CTBs. Therefore, a high density of dislocations can be accumulated in regions confined by the CTBs which led to strong strain hardening.

4.2. Influences of surface groove on dislocation nucleation site under uniaxial deformation

It was shown in both Figs. 2 and 5 that the surface groove has little effect on the dislocation nucleation site at the yielding of FT Ag NWs under uniaxial deformation. For example, Figs. 2c and 5b and c showed that in spite of the presence of surface groove the yielding in these NWs occurred via the nucleation of partial dislocations from the intersection between CTBs and NW surface. Such site-specific dislocation nucleation phenomenon has been found previously in periodically twinned metal NWs under uniaxial tension and it was found that those dislocation sites were locations of the highest stress (σ_{zz}) gradient [31]. The initial axial stress distribution among different NWs in Fig. 1c showed that although the presence of a surface groove would relax the internal compressive stress of FT Ag NW, the overall stress distribution pattern remained relatively unchanged. Therefore, the preference of dislocation nucleation sites was not considerably influenced. Nevertheless, it is important to mention that the dislocation nucleation sites can be changed in FT Ag NWs by varying the NW diameter and temperature under both uniaxial tension and compression [32].

5. Conclusions

In summary, MD simulations of uniaxial deformation and nanoindentation were performed to systematically investigate the synergistic effects from both internal and external structural defects on the yielding and plasticity of Ag NWs. It was found that the structural defects, including fivefold CTBs, surface facets, and

surface groove can dramatically alter the initial stress state in Ag NWs prior to mechanical deformation. As a result, the internal fivefold CTBs and external surface facets can dramatically influence the yielding of Ag NWs under uniaxial deformation, which can change not only the preferred dislocation nucleation site but also the stress level at which the Ag NWs yielded. It was found that both the fivefold CTBs and surface facets led to strengthening under tension but weakening under compression in Ag NWs. With the presence of a surface groove, however, such strengthening or weakening effects were mitigated by partially relaxing the initial compressive stress in FT Ag NWs. On the other hand, fivefold CTBs can serve as strong barriers to dislocation motion in FT Ag NWs under nanoindentation, thus resulting in significant strain hardening. Moreover, an unusual oscillation behavior was observed in FT Ag NWs with surface groove which was associated with the “opening-and-closing” of the surface groove during nanoindentation. Our study provides the in-depth understanding of the microstructure–property relationship in metal NWs and should shed light in the design of novel one-dimensional nanostructures.

Acknowledgements

This work was supported by Fudan University, China and the University of Manitoba, Canada.

Appendix A. Supplementary material

Supplementary data associated with this article can be found, in the online version, at <http://dx.doi.org/10.1016/j.commatsci.2013.06.021>.

References

- [1] G.A. Ozin, I. Manners, S. Fournier-Bidoz, A. Arsenault, *Advanced Materials* 17 (2005) 3011–3018.
- [2] D.C. Meier, S. Semancik, B. Button, E. Strelcov, A. Kolmakov, *Applied Physics Letters* 91 (2007). 063118–063118.
- [3] Y. Li, F. Qian, J. Xiang, C.M. Lieber, *Materials Today* 9 (2006) 18–27.
- [4] J.H. He, P.H. Chang, C.Y. Chen, K.T. Tsai, *Nanotechnology* 20 (2009) 135701.
- [5] Y. Zhu, Q. Qin, F. Xu, F. Fan, Y. Ding, T. Zhang, et al., *Physical Review B* 85 (2012) 045443.
- [6] J.R. Greer, J.T.M. De Hosson, *Progress in Materials Science* 56 (2011) 654–724.
- [7] C. Deng, F. Sansoz, *Nano Letters* 9 (2009) 1517–1522.
- [8] C. Deng, F. Sansoz, *ACS Nano* 3 (2009) 3001–3008.
- [9] J. Diao, K. Gall, M.L. Dunn, J.A. Zimmerman, *Acta Materialia* 54 (2006) 643–653.
- [10] F. Sansoz, *Acta Materialia* 59 (2011) 3364–3372.
- [11] B. Wu, A. Heidelberg, J.J. Boland, J.E. Sader, Sun, Li, *Microstructure-hardened silver nanowires*, *Nano Lett.* 6 (2006) 468–472.
- [12] Y. Gao, L. Song, P. Jiang, L.F. Liu, X.Q. Yan, Z.P. Zhou, et al., *Journal of Crystal Growth* 276 (2005) 606–612.
- [13] W. Zhang, Y. Liu, R. Cao, Z. Li, Y. Zhang, Y. Tang, et al., *Journal of the American Chemical Society* 130 (2008) 15581–15588.
- [14] Y.G. Zheng, H.W. Zhang, Z. Chen, L. Wang, Z.Q. Zhang, J.B. Wang, *Applied Physics Letters* 92 (2008). 041913–041913.
- [15] Y.T. Zhu, X.Z. Liao, R.Z. Valiev, *Formation mechanism of fivefold deformation twins in nanocrystalline face-centered-cubic metals*, *Applied Physics Letters* 86 (2005) 103112–1–103112–3.
- [16] X. Fu, J. Jiang, W. Zhang, J. Yuan, *Incoherent structural relaxation of fivefold twinned nanowires*, *Applied Physics Letters* 93 (2008) 043101–1–043101–3.
- [17] A.T. Jennings, J.R. Greer, *Journal of Materials Research* 26 (2011) 2803–2814.
- [18] L. Lu, Y. Shen, X. Chen, L. Qian, K. Lu, *Science* 304 (2004) 422–426.
- [19] C. Deng, F. Sansoz, *Fundamental differences in the plasticity of periodically twinned nanowires in Au, Ag, Al, Cu, Pb and Ni*, *Acta Materialia* 57 (2009) 6090–6101.
- [20] J.Y. Wu, S. Nagao, J.Y. He, Z.L. Zhang, *Nano Letters* 11 (2011) 5264–5273.
- [21] Y. Gao, Y. Fu, W. Sun, Y. Sun, H. Wang, F. Wang, et al., *Computational Materials Science* 55 (2012) 322–328.
- [22] Y.-H. Wen, R. Huang, Z.-Z. Zhu, Q. Wang, *Computational Materials Science* 55 (2012) 205–210.
- [23] A.M. Leach, M. McDowell, K. Gall, *Advanced Functional Materials* 17 (2007) 43–53.
- [24] F. Sansoz, V. Dupont, *Scripta Materialia* 63 (2010) 1136–1139.
- [25] V. Dupont, F. Sansoz, *Journal of Materials Research* 24 (2009) 948–956.
- [26] S. Plimpton, *Journal of Computational Physics* 117 (1995) 1–19.
- [27] P.L. Williams, Y. Mishin, J.C. Hamilton, *Modelling and Simulation in Materials Science and Engineering* 14 (2006) 817–833.

- [28] J. Li, *Modelling and Simulation in Materials Science and Engineering* 11 (2003) 173.
- [29] J. Diao, K. Gall, M.L. Dunn, *Nano Letters* 4 (2004) 1863–1867.
- [30] D.-L. Chen, T.-C. Chen, *Nanotechnology* 16 (2005) 2972.
- [31] C. Deng, F. Sansoz, *Applied Physics Letters* 95 (2009). 091914-091914.
- [32] M. Sun, R. Cao, F. Xiao, C. Deng, Five-fold twin and surface groove-induced abnormal size- and temperature-dependent yielding in Ag nanowires, *Scripta Materialia* (2013) 227–230.